Cell

SARAF Inactivates the Store Operated Calcium Entry Machinery to Prevent Excess Calcium Refilling

Raz Palty,[1] Adi Raveh,[1] Ido Kaminsky,[1] Ruth Meller,[1] and Eitan Reuveny[1,*]
[1]Department of Biological Chemistry, Weizmann Institute of Science, Rehovot 76100, Israel
*Correspondence: e.reuveny@weizmann.ac.il
DOI 10.1016/j.cell.2012.01.055

SUMMARY

Store operated calcium entry (SOCE) is a principal cellular process by which cells regulate basal calcium, refill intracellular Ca^{2+} stores, and execute a wide range of specialized activities. STIM and Orai proteins have been identified as the essential components enabling the reconstitution of Ca^{2+} release-activated Ca^{2+} (CRAC) channels that mediate SOCE. Here, we report the molecular identification of SARAF as a negative regulator of SOCE. Using heterologous expression, RNAi-mediated silencing and site directed mutagenesis combined with electrophysiological, biochemical and imaging techniques we show that SARAF is an endoplasmic reticulum membrane resident protein that associates with STIM to facilitate slow Ca^{2+}-dependent inactivation of SOCE. SARAF plays a key role in shaping cytosolic Ca^{2+} signals and determining the content of the major intracellular Ca^{2+} stores, a role that is likely to be important in protecting cells from Ca^{2+} overfilling.

INTRODUCTION

Store operated calcium entry (SOCE) represents a key mechanism, by which cells convey Ca^{2+} signals and maintain Ca^{2+} homeostasis (Parekh and Putney, 2005). Despite its initial characterization more than two decades ago, when SOCE was characterized mainly via mechanistic and biophysical means, only recently have the molecular components essential for its activity been identified. The molecular identification revealed the discrete events associated with SOCE activation and regulation (Cahalan, 2009; Lewis, 2007; Putney, 1986). STIM and Orai proteins are the essential components that enable the reconstitution of Ca^{2+} release-activated Ca^{2+} (CRAC) channels underlying SOCE activity (Feske et al., 2006; Liou et al., 2005; Peinelt et al., 2006; Prakriya et al., 2006; Roos et al., 2005; Soboloff et al., 2006; Vig et al., 2006; Zhang et al., 2006; Zhang et al., 2005). Although other proteins, such as members of the TRPC family, might also be involved in SOCE (Hardie and Minke, 1993; Kiselyov et al., 1998; Liu et al., 2007; Pani et al., 2009), STIM, the Ca^{2+} sensor (Liou et al., 2005; Roos et al., 2005; Stathopulos et al., 2008; Zhang et al., 2005), and Orai, the channel pore forming subunit (Prakriya et al., 2006; Vig et al., 2006; Yeromin et al., 2006), have been shown to be sufficient for this activity. STIM is an endoplasmic reticulum (ER) single pass membrane protein (Hogan et al., 2010), which detects changes in ER Ca^{2+} levels through a conserved Ca^{2+} binding domain (EF hand) (Stathopulos et al., 2009; Stathopulos et al., 2008). ER Ca^{2+} depletion leads to STIM oligomerization and relocalization to specialized regions close to the plasma membrane (ER-PM junctions), where it directly binds to Orai, causing the opening of the channel and initiation of Ca^{2+} entry (Baba et al., 2006; Barr et al., 2008; Frischauf et al., 2009; Kawasaki et al., 2009; Liou et al., 2007; Liou et al., 2005; Muik et al., 2008; Navarro-Borelly et al., 2008; Park et al., 2009; Wu et al., 2006; Yuan et al., 2009; Zhang et al., 2005; Zhou et al., 2010). Once SOCE is activated, it is subjected to various direct and indirect regulatory processes that determine the duration and magnitude of the Ca^{2+} influx, which set downstream cellular events (Hogan et al., 2010; Parekh and Putney, 2005). Two definitive Ca^{2+}-dependent modes of regulation of CRAC channels were previously reported: fast inactivation that depends largely on STIM1 and calmodulin binding to Orai1 (Derler et al., 2009; Hoth and Penner, 1993; Lee et al., 2009; Litjens et al., 2004; Mullins et al., 2009) and a slow Ca^{2+}-dependent inactivation process with an unknown molecular mechanism (Louzao et al., 1996; Parekh, 1998; Zweifach and Lewis, 1995).

Using a functional-based high-throughput screen, we have identified the gene product of *TMEM66*, named hereafter as SARAF (for SOCE-associated regulatory factor) as a regulator of cellular Ca^{2+} homeostasis. SARAF is a highly conserved protein in vertebrates and has poor functional annotation. In mammals, SARAF is ubiquitously expressed but has exceptionally high transcript levels in the immune and neuronal tissues (Su et al., 2004). In this study we show that SARAF is an ER resident protein, which responds to cytosolic Ca^{2+} elevation after ER Ca^{2+} refilling by promoting a slow inactivation process of STIM2-dependent basal SOCE activity, as well as STIM1-mediated SOCE activity. These actions collectively impose stringent conditions for maintaining proper intracellular Ca^{2+} levels in both resting and stimulated cells.

RESULTS

SARAF Regulates Basal ER and Cytosolic Ca^{2+} Levels

We performed a functional expression screen in an attempt to isolate cDNA candidates that affect mitochondrial Ca^{2+} homeostasis (Figures S1A and S1B, available online). These efforts lead to the identification of a ~2 kilobase cDNA clone with a 1020 bp open reading frame coding for SARAF (accession #JQ348891) (also known as TMEM66, XTP-3, FOAP-7, HSPC035, MGC8721 or FLJ22274) (Figure 1A). Transfection of HEK293 cells with SARAF cDNA alone resulted in lowered basal mitochondrial Ca^{2+} levels compared to control cells (Figures S1A and S1B).

Because changes in basal mitochondrial Ca^{2+} levels may reflect changes in global cellular Ca^{2+} homeostasis, we also tested the effect of SARAF expression on cytosolic and ER Ca^{2+} levels. These parameters were measured with a fura-2 or FRET-based D1ER indicator (Palmer et al., 2004), respectively. Transfection of HeLa or HEK293-T cells with SARAF cDNA, or with an empty vector (control), showed that basal $[Ca^{2+}]_{ER}$ was significantly decreased in SARAF-overexpressing cells (Figure 1B). In order to assess the relationship between SARAF expression levels and $[Ca^{2+}]_{cyto}$, we expressed SARAF C terminally tagged with yellow fluorescent protein (YFP) (SARAF-YFP) or YFP (control), and measured $[Ca^{2+}]_{cyto}$ as a function of protein expression, as judged by YFP fluorescence. We found that decreased $[Ca^{2+}]_{cyto}$ highly correlated with YFP fluorescence in cells expressing SARAF-YFP but not in cells expressing YFP alone (Figure 1C), indicating that SARAF expression primarily affected global Ca^{2+} homeostasis. In order to assess the role of endogenous SARAF expression, a siRNA silencing approach against SARAF was used in both HeLa and Jurkat cells. Reduced expression of SARAF resulted in a significant elevation of basal $[Ca^{2+}]_{cyto}$ in both cell types (Figures 1D–1F). Likewise, $[Ca^{2+}]_{ER}$ levels, estimated by organelle content release using ionomycin (Brandman et al., 2007) or with the D1ER indicator, were higher in siRNA-treated cells, (Figure 1F inset and Figure S1D). The specificity and efficiency of siRNA-mediated silencing of SARAF mRNA and protein levels were determined by western blotting, semiquantitative RT-PCR, and a fluorescent-based assay employing YFP fluorescence as reference for protein expression (Figure 1D and Figure S2). The functionality of SARAF-YFP suggested that the protein is correctly expressed and folded and therefore encouraged us to study its cellular localization. When a fluorescent-tagged chimera of SARAF was coexpressed with either that of STIM1 or SEC61, both ER resident proteins, SARAF fluorescence strongly overlapped with both markers (Figure 1G and Figure S1E), but did not colocalize with that of mitochondrial markers (data not shown), indicating that the ER is the primary site for SARAF subcellular localization.

At resting conditions, SARAF modulation of $[Ca^{2+}]_i$ must involve a change of Ca^{2+} fluxes at the level of the plasma membrane (Ríos, 2010). This can be achieved either through the regulation of plasma membrane Ca^{2+} permeation or extrusion pathways. In order to distinguish between these two possibilities, we overexpressed SARAF in HEK293-T or HeLa cells and tested whether SARAF-mediated reduction of $[Ca^{2+}]_{cyto}$ depended on the presence of Ca^{2+} in the growth media. Control and SARAF overexpressing cells grown on a low Ca^{2+}-containing media (0.1 mM), exhibited similar cytosolic Ca^{2+} levels (Figure S1C), suggesting that increased SARAF expression is linked to inhibition of Ca^{2+} entry from an extracellular source rather than the activation of a Ca^{2+}-extrusion mechanism. Recent findings by Meyer and colleagues showed that STIM2 plays a central role in maintaining basal $[Ca^{2+}]_{cyto}$ and $[Ca^{2+}]_{ER}$ by acting as a feedback regulator that senses small changes in ER Ca^{2+} and translates them into differential gating of Orai1 (Brandman et al., 2007). To test whether SARAF regulation of basal $[Ca^{2+}]_{cyto}$ is linked to the STIM2-Orai1 pathway, we used siRNA-mediated knock down of STIM2, either alone, or together with SARAF, and determined basal $[Ca^{2+}]_{cyto}$ in HeLa cells. In agreement with previous studies (Bird et al., 2009; Brandman et al., 2007), we observed a significant decrease in $[Ca^{2+}]_{cyto}$ after STIM2 silencing, compared to control (Figure 1H). More importantly, silencing both STIM2 and SARAF did not result in an additive effect on resting $[Ca^{2+}]_{cyto}$. These results suggest that SARAF, with STIM2, may act on a similar Ca^{2+} permeation pathway.

SARAF Regulates STIM1-Orai1-Mediated Store Operated Calcium Entry

STIM2 and STIM1 share moderate sequence similarity and maintain similar domain architecture (Hogan et al., 2010). To test whether SARAF regulates STIM1-Orai1-mediated SOCE, we heterologously expressed STIM1 and Orai1 alone or with SARAF in HEK293 or HEK293-T cells and measured I_{CRAC}, with the whole-cell variation of the patch clamp technique by passively depleting Ca^{2+} from the ER by using ethylene glycol-bis(2-aminoethylether)-N,N,N′,N′-tetraacetic acid (EGTA) (1.2 mM) in the recording pipette (Zweifach and Lewis, 1995). After 3 min under whole-cell configuration in zero extracellular Ca^{2+}, addition of 10 mM Ca^{2+} to the bath solution initiated La^{3+}-sensitive strong inwardly rectifying currents typical of I_{CRAC} (Figures S2A and S2B). These had similar magnitudes in both control- expressing (HEK293 22.6 ± 2 pA/pF and HEK239-T 40.7 ± 3.5 pA/pF) and SARAF- expressing (HEK293 27.1 ± 6pA/pF and HEK293-T 41.8 ± 3.3 pA/pF) cells. Strikingly, we found clear differences in current inactivation. In control HEK293 cells, currents partially inactivated to steady-state levels (35.6% ± 3.2% of peak levels), whereas in SARAF-expressing cells, the extent of current inactivation was greatly increased (17.3% ± 1% of peak levels, Figure 2A). An additional period of passive store depletion, when no external Ca^{2+} was present, partially restored I_{CRAC} in control cells (46.5% ± 4.7% of peak levels), whereas in SARAF-expressing cells, currents remained inactivated (21% ± 3% of peak levels). These results indicate that part of the SARAF-mediated I_{CRAC} inhibition does not require the continuous presence of elevated Ca^{2+}. Similar results were also obtained from HEK293-T cells under the same experimental conditions (Figures S3A and S3B). Intriguingly, a similar "slow inactivation" process of native I_{CRAC} currents in Jurkat T-lymphocytes and RBL cells has been observed (Parekh, 1998; Zweifach and Lewis, 1995); however, the molecular component responsible for this process remained unknown. The continuous nature of the SARAF-mediated I_{CRAC} inhibition suggests that inhibition may be Ca^{2+} dependent. We therefore performed similar experiments as described above using the

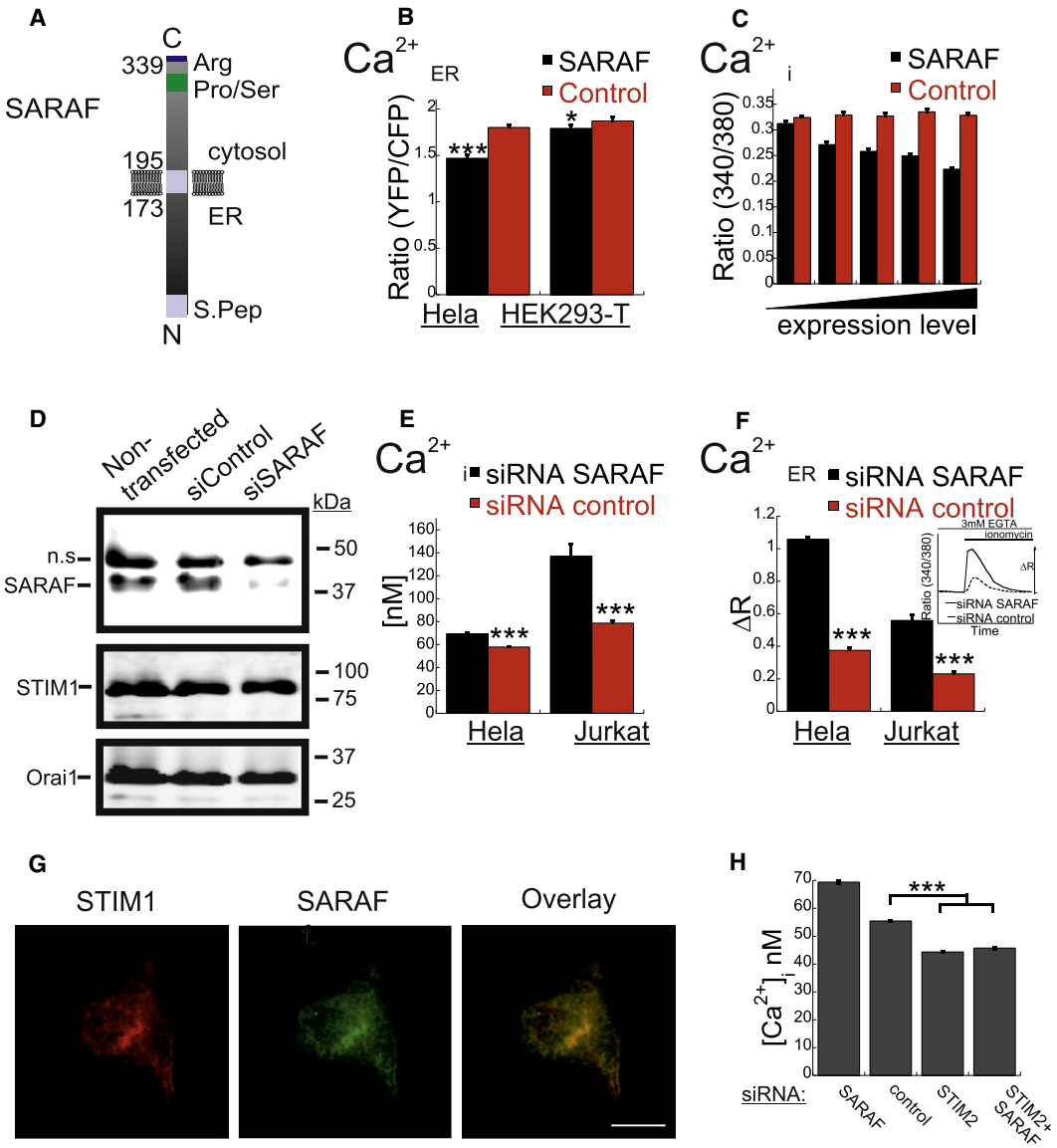

Figure 1. SARAF Regulates Basal Cytosolic and ER Ca^{2+} Concentrations by Inhibiting STIM2-Dependent Basal SOCE

(A) The predicted topology and domain structure of the human SARAF. Human SARAF has 339 amino acids with a validated signal peptide (S.Pep) (1–30 [Zhang and Henzel, 2004]) and a putative single membrane spanning domain (173–195, predicted by the SOSUI program). Initiation point of SARAF short isoform is indicated (aa 173). Also marked are clusters of serine/proline (284–310) and arginine rich regions.

(B) ER Ca^{2+} levels were measured in control and heterologously expressing SARAF cells, together with D1ER. Averaged D1ER emission ratios from individual cells are shown (HEK293-T [control, n = 76; SARAF, n = 86], HeLa [control, n = 71; SARAF n = 61]).

(C) Cytosolic Ca^{2+} levels and YFP expression were measured in HEK293-T cells transfected with SARAF-YFP or YFP (control). Expression units that cover the entire YFP fluorescence range were created by grouping 35–50 cells distributed around similar YFP fluorescent values (SARAF-YFP, n = 228; control-YFP, n = 217). The averaged basal Ca^{2+} levels are plotted as a function of expression groups.

(D) Immunoblot analysis of SARAF, STIM1 and Orai1 expressed in HeLa cells before or after treatment with siSARAF or siGFP (control).

(E) Cytosolic Ca^{2+} levels of HeLa cells transfected with siSARAF (n = 118) or siGFP (n = 185), and of Jurkat cells (siSARAF, n = 236) (siGFP, n = 247).

(F) Averaged ER Ca^{2+} measured in individual cells transfected with siSARAF or siControl (nontarget, see Extended Experimental Procedures). ER Ca^{2+} was estimated by monitoring the peak of ionomycin-induced Ca^{2+} released from the ER in the presence of extracellular EGTA (3 mM, inset).

(G) Fluorescent images of a HEK293-T cell expressing SARAF-GFP (green) and STIM1-mCherry (red); the scale bar represents10 μm. (H) Cytosolic Ca^{2+} levels of HeLa cells transfected siSARAF (n = 250), si STIM2 (n = 417), siSTIM2+siSARAF (n = 481), or siControl (n = 289). p value: * < 0.05, ** < 0.01, *** < 0.001.

faster Ca^{2+} chelator, 1,2-bis(o-aminophenoxy)ethane-N,N,N',N'-tetra-acetic acid (BAPTA) (10 mM), in the pipette solution. Under these experimental conditions, I_{CRAC} currents were of similar magnitude for both control and SARAF-expressing cells and did not undergo inactivation (Figure 2B). These results suggest that the onset of SARAF-mediated I_{CRAC} inactivation depends

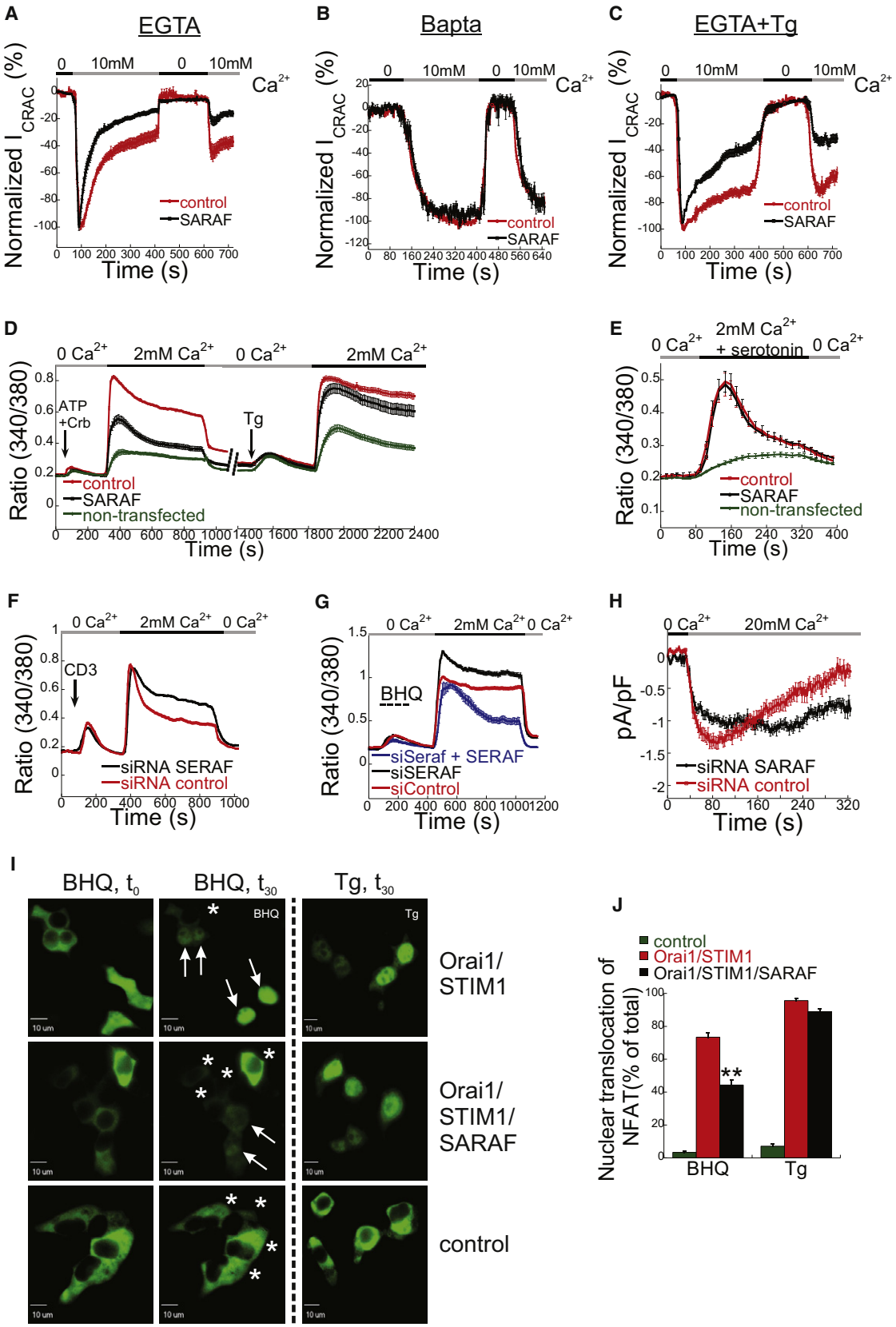
A
EGTA
B
Bapta
C
EGTA+Tg
Normalized I CRAC (%)
0 10mM 0 10mM Ca2+
control
SARAF
Time (s)
D
0 Ca2+ 2mM Ca2+ 0 Ca2+ 2mM Ca2+
ATP +Crb
Tg
non-transfected
Ratio (340/380)
E
0 Ca2+ 2mM Ca2+ + serotonin 0 Ca2+
F
0 Ca2+ 2mM Ca2+ 0 Ca2+
CD3
siRNA SERAF
siRNA control
G
BHQ
siSeraf + SERAF
siSERAF
siControl
H
0 Ca2+ 20mM Ca2+
pA/pF
siRNA SARAF
I
BHQ, t0
BHQ, t30
Tg, t30
Orai1/ STIM1
Orai1/ STIM1/ SARAF
control
10 um
J
control
Orai1/STIM1
Orai1/STIM1/SARAF
Nuclear translocation of NFAT(% of total)
**
BHQ
Tg

on the presence of free cytosolic Ca^{2+} ions. To address more specifically whether ER luminal Ca^{2+} content affects SARAF-mediated I_{CRAC} inhibition, we repeated the experimental paradigm as in Figure 2A with the addition of 2 μM Thapsigargin (Tg), an irreversible SERCA (sarcoplasmic/endoplasmic reticulum Ca^{2+}-ATPase), in the patch pipette solution. In the absence of ER Ca^{2+} refilling, both control and SARAF-expressing cells exhibited reduced I_{CRAC} inactivation (Figure 2C) compared to conditions that allow ER Ca^{2+} refilling (Figure 2A), indicating that store refilling partially contributes to the inactivation process. In the absence or presence of Tg, the extent of current inactivation in control cells was 35.6% ± 3.2% (from Figure 2A) and 80.6% ± 4.4% of peak levels, respectively. Similar changes were seen in cells expressing SARAF, with 17.3% ± 1% (from Figure 2A) and 40% ± 1.6% of peak levels, respectively. These data suggest that there is a substantial component of I_{CRAC} inactivation that is dependent on luminal Ca^{2+}, which in turn may be partially modulated by SARAF. In order to further confirm that SARAF is indeed involved in regulating Ca^{2+} entry upon ER Ca^{2+} depletion, we monitored SOCE-induced $[Ca^{2+}]_i$ changes under conditions that either allowed or prevented ER refilling. To equilibrate both $[Ca^{2+}]_{cyto}$ and $[Ca^{2+}]_{ER}$ in control and SARAF-expressing cells, we incubated cells in a Ca^{2+}-free extracellular solution (1 mM EGTA) (Brandman et al., 2007) for 45 min prior to the initiation of experiment. Transient ER Ca^{2+} depletion was induced by bath application of 100 μM ATP and 100 μM carbachol (Carb) (Figure 2D). In cells coexpressing Orai1, STIM1, and SARAF, the rise in $[Ca^{2+}]_{cyto}$ after the addition of extracellular Ca^{2+} was about 2-fold lower than in STIM1- and Orai1-coexpressing cells (Figure 2D). In contrast, under conditions where SOCE activity was induced by Tg, the apparent ability of SARAF to inhibit SOCE activity was greatly diminished. It should be noted that a small but persistent difference in $[Ca^{2+}]_{cyto}$ rise under these conditions was maintained between SARAF-expressing and control cells (an average of 13.9% ± 2.2% in the relative R_{max} value, from seven independent experiments, $p < 0.05$, t test analysis). The apparent nonlinear correlation between the effects of SARAF on steady-state I_{CRAC} currents and on $[Ca^{2+}]_{cyto}$ may arise because of the nature of the recording method, i.e., direct Ca^{2+} ion flow versus cumulative determination $[Ca^{2+}]_{cyto}$ with electrophysiology and fluorescence Ca^{2+} imaging, respectively. Nevertheless, to exclude the possibility that SARAF somehow interfered nonspecifically with cellular Ca^{2+} signaling, we monitored the serotonin-dependent Ca^{2+} influx through the 5HT3 receptor (5HT3R), in HEK293-T cells. SARAF expression did not affect 5HT3R-mediated Ca^{2+} influx and thus a nonspecific effect of SARAF on Ca^{2+} permeation is ruled out (Figure 2E). To substantiate that indeed SARAF is playing an important role in regulating SOCE activity under native conditions, we measured SOCE activity in Jurkat T cells where endogenous SARAF levels were reduced by siRNA. In these cells, we performed both transient activation of SOCE (using anti-CD3) and permanent activation (using Tg) by using a similar experimental paradigm to that described in Figure 2D (Figure 2F and Figure S3E). SOCE activation by CD3-induced store depletion in siSARAF-treated Jurkat cells resulted in prolonged elevation of $[Ca^{2+}]_{cyto}$, whereas control cells exhibited similar initial Ca^{2+} elevation, which later decreased to levels that were about 2-fold lower than in SARAF-silenced cells. SOCE induction by Tg showed no significant differences between control and siSARAF-treated cells, which is similar to the experiments with HEK293 cells (Figure S3E). Similar results were also obtained from HeLa cells in which SARAF expression was either elevated via SARAF cDNA expression or reduced by siSARAF (Figures S3C and S3D), thus emphasizing the ubiquitous nature of SARAF action. To confirm that endogenous SARAF was indeed the molecular component responsible for SOCE inactivation, we tested the ability of the murine form of SARAF (mSARAF), whose mRNA is not targeted by the human siSARAF used in the above experiments (Figure S2F), to rescue the SARAF phenotype. Jurkat cells were cotransfected with siSARAF with or without mSARAF cDNA, and SOCE was activated by the reversible SERCA inhibitor BHQ (2,5-Di-t-butyl-1,4-benzohydroquinone). mSARAF rescued SOCE inactivation, indicating that SARAF is the molecular component responsible for SOCE inactivation (Figure 2G and Figures S3F–S3H). Similarly, recording of I_{CRAC} from Jurkat cells treated with siSARAF also showed a reduction in current inactivation; in control cells, currents remaining after 4 min in the presence of high external Ca^{2+} were 15.2% ± 5% (n = 15), whereas in siSARAF-treated cells, currents were 82% ± 4% (n = 9, $p < 0.05$) (Figure 2H). Current densities in control and siSARAF-treated Jurkat cells, however, were similar, with values of 1.35 ± 0.10 pA/pF and 1.17 ± 0.06 pA/pF, respectively.

Figure 2. SARAF Mediates ER Ca^{2+} Refilling-Dependent Regulation of SOCE

(A–C) Normalized whole cell current levels at −100 mV of cells expressing YFP-STIM1, mCherry-Orai1 with (black) or without SARAF (red). (A) Pipette solutions contained (A) 1.2 mM EGTA, SARAF (n = 6), control (n = 9) (B) 10 mM Bapta, SARAF (n = 6), control (n = 8) (B), or (C) 1.2 mM EGTA plus 0.2 μM Tg, SARAF (n = 11), control (n = 9).

(D) Mean intracellular Ca^{2+} traces recorded from individual cells (SARAF, n = 36; control, n = 46) after activation of SOCE by ATP + Charbachol (100 μM each) or Tg (0.2 μM).

(E) Analysis of 5-HT3 ionophoric receptor activity (1 μM serotonin) expressed with (n = 11, black), without SARAF (n = 14, red) or nontransfected (n = 8, green) in HEK293-T; response was triggered by 1 μM of serotonin in the presence of 2 mM Ca^{2+}.

(F) Average CD3-induced SOCE activity in Jurkat T cells transfected with siSARAF (n = 45, black) or nontarget siControl (n = 52, red).

(G) Averaged BHQ-induced SOCE response in Jurkat T cells transfected with siSARAF (black, n = 41), siSARAF with mouse-siSARAF (blue, n = 15) and nontarget siControl (red, n = 44).

(H) Averaged whole cell I_{CRAC} currents at −100 mV recorded from Jurkat T cells treated with siSARAF (black, n = 9) or siControl (red, n = 15). Pipette solutions containing 1.2 mM EGTA.

(I) Representative fluorescent images of GFP-NFAT localization in HEK293-T cells expressing GFP-NFAT (control), with STIM1/Orai1 or with STIM1/Orai1/SARAF. Arrows indicate cells with nuclear localization and asterisks indicate cytosolic localization of NFAT.

(J) Quantitation of GFP-NFAT nuclear localization in transfected cell (as in I) Tg- (n = 2) and BHQ-induced SOCE(n = 6). (n = number of independent experiments, 60–100 cells analyzed in each experiment). p value: * < 0.05, ** < 0.01.

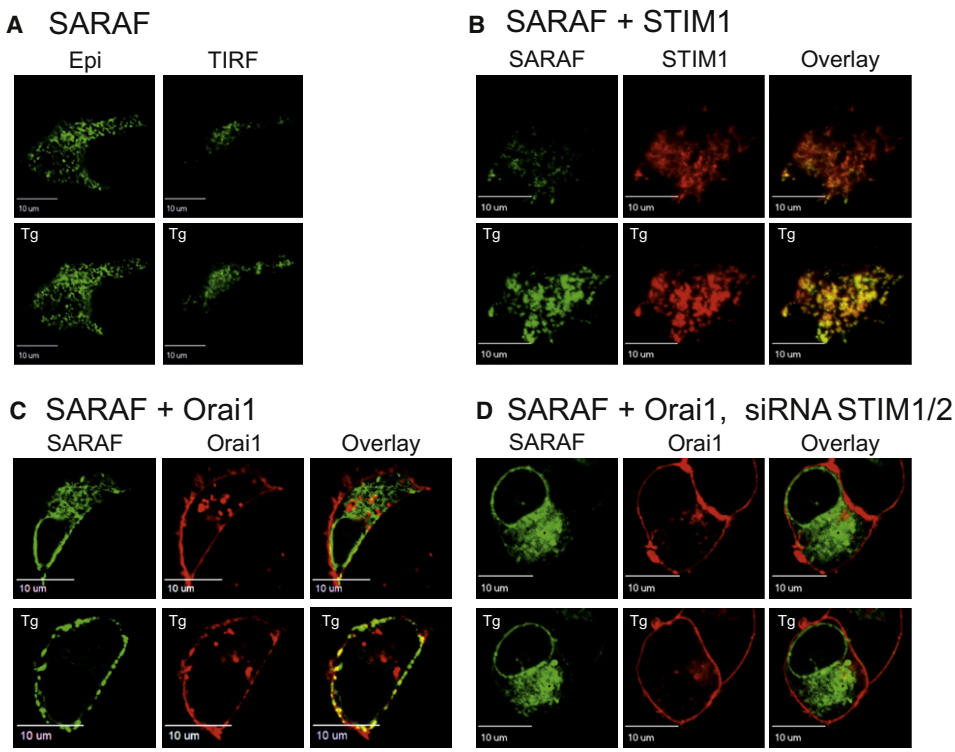

Figure 3. SARAF Translocates to ER-PM Regions in a STIM1-Dependent Manner after Store Depletion

(A) Fluorescent images of an HEK293 cell expressing SARAF-GFP, taken under epi illumination or TIRF configurations. Images of the same cell taken after the application of Tg (0.2 μM) (lower).

(B) TIRF images of a cell expressing SARAF-GFP and STIM1-mCherry before (upper) and after incubation with Tg (lower).

(C) Images of a cell expressing SARAF-GFP and Orai-mCherry, taken under epi illumination, before (upper) and after the application of Tg (lower).

(D) Images of a cell expressing SARAF-GFP, Orai-mCherry treated with siSTIM1 and siSTIM2, taken under epi illumination, before (upper) and after the application of Tg (lower).

As an independent third measure for the possible action of SARAF on SOCE activity, we assessed the ability of SARAF to interfere with the Ca^{2+}-dependent translocation of the nuclear factor of activated T cells (NFAT-GFP) to the cell nucleus (Tomida et al., 2003). In unstimulated cells, coexpressing STIM1 and Orai1 with or without SARAF, NFAT-GFP was predominantly found in the cytoplasm. After ER Ca^{2+} depletion by BHQ and the reintroduction of external Ca^{2+}, in cells expressing STIM1 and Orai1, 73% ± 2.8% of the cells exhibited nuclear NFAT-GFP localization, compared to only 44% ± 3.1% of the cells expressing STIM1, ORAI1, and SARAF. In contrast, when ER refilling was abolished by Tg, nearly all cells exhibited nuclear localization of NFAT and the expression of SARAF no longer made a significant difference (Figures 2I and 2J). The experiments described above indicate that SARAF-mediated SOCE inactivation primarily depends on cytosolic Ca^{2+} rise and is partially affected by the ER Ca^{2+} refilling state.

SARAF Translocates to ER-PM Regions in a STIM1-Dependent Manner after Store Depletion

One of the most prominent manifestations of STIM1-Orai1-induced SOCE is the puncta formation of a multimeric STIM1-Orai1 protein aggregate at specialized ER-PM junctions (Liou et al., 2005). If SARAF directly inhibits SOCE, it should be found at these active sites as well. Indeed, in cells coexpressing SARAF-GFP together with STIM1-mCherry and Orai1, but not in cells expressing SARAF-GFP alone, upon depletion of ER stores with Tg, a significant translocation of SARAF-GFP and STIM1-mCherry to the plasma membrane was apparent (Figure 3A–3C and Movie S1). SARAF-GFP translocation into ER-PM regions did not depend on the $[Ca^{2+}]_{cyto}$ because chelation of free cytosolic Ca^{2+} did not prevent it (Figure S4D). These results indicate that ER depletion alone is not sufficient for SARAF translocation and that either Orai1 or STIM1 were essential for this process. To test whether endogenous STIM played a role in the Tg-induced SARAF translocation, we coexpressed SARAF-GFP and Orai1-mCherry in siSTIM1 and siSTIM2-treated cells (Figures S4A–S4C) and monitored their cellular localization. Silencing STIM1 and STIM2 protein levels inhibited the Tg-induced SARAF-GFP translocation in the presence of Orai1-mCherry (Figure 3D). These results indicate that after store depletion, SARAF ability to translocate into ER-PM regions depends primarily on the presence of STIM proteins.

SARAF Luminal Domain Regulates Its Activity and the Cytosolic Domain Is Responsible for SOCE Modulatory Function

Full-length human SARAF cDNA encodes a 339 amino acid (aa) protein that contains a cleavable signal peptide (aa 1–30)

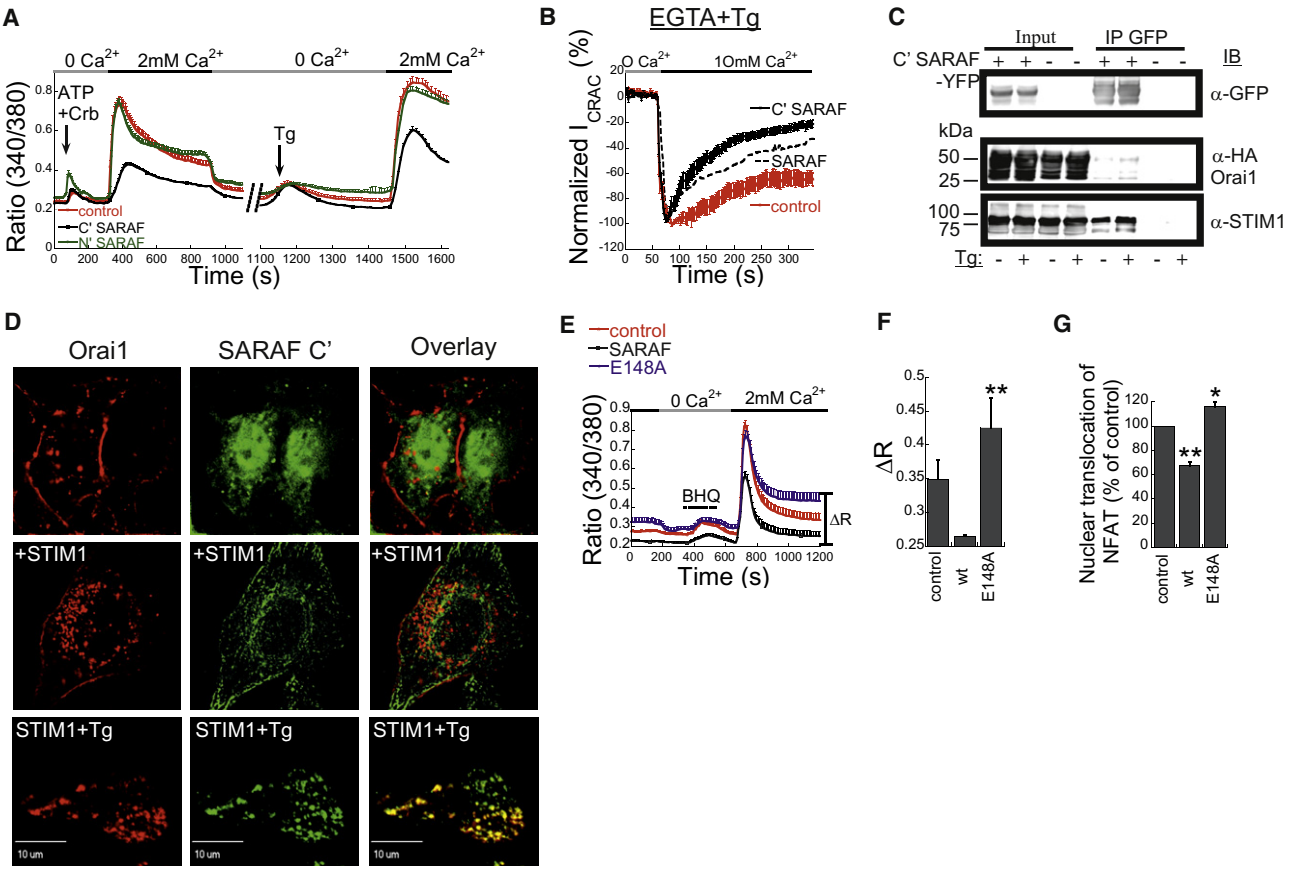

Figure 4. The ER Luminal Domain of SARAF Regulates Its Activity and the Cytosolic Domain Mediates Its SOCE Inhibitory Activity

(A) Mean intracellular Ca^{2+} traces of individual HEK293-T cells expressing STIM1+Orai1 alone (n = 46) or with N′ (SARAF(1-191)) (n = 38) or C′ (SARAF(196-339)) (n = 29) termini of SARAF constructs. SOCE was induced by ATP+Charbachol (100 μM each) or Tg (0.2 μM).

(B) Mean normalized whole-cell I_{CRAC} currents (at −100 mV, 1.2 mM EGTA, and 2 μM Tg in the pipette) of cells expressing STIM1 and Orai1 with (black, n = 8) or without C′-SARAF-GFP (n = 14). Dashed trace is taken from Figure 2C for comparison.

(C) Western blot analysis of input or immune-precipitated material (IP with anti-GFP) prepared from cells expressing Orai1and STIM1 before and after SOCE induction by Tg, supplemented with purified YFP-SARAF(196-339) or GIRK1(365-501) (negative control) proteins.

(D) Fluorescent images of HEK293-T cells coexpressing YFP-C′-SARAF and mCherry-Orai1 alone or with STIM1. (Lower) TIRF images of a cell expressing mCherry-Orai1/STIM1/YFP-C′ SARAF after SOCE induction.

(E) Mean intracellular Ca^{2+} traces of individual HEK293-T cells expressing STIM1+Orai1 alone (red), with SARAF (black), or with SARAF(E148A) mutant (blue). SOCE was induced with BHQ (2 μM) as indicated.

(F) Quantitation of steady-state SOCE activity (ΔR) as indicated in (E), data obtained from three independent experiments (15–45 cells each).

(G) Normalized percentage of GFP-NFAT nuclear localization induced by BHQ in cells expressing STIM1/Orai1 alone, with SARAF, or SARAF(E148A). Data obtained from three independent experiments (60–100 cells each). p values: * < 0.05, ** < 0.01, *** < 0.001.

(Zhang and Henzel, 2004) and a single putative transmembrane domain (aa 173–195). SARAF topology predicts a cytoplasm facing domain (aa 196–339) and an ER-luminal facing domain (aa 31–172) (Figure 1A). We cloned an additional splice isoform of the human SARAF gene, SARAF-S, from HEK293 cells (accession number JQ348892). This splice isoform lacks the second exon of the full-length SARAF and results in a shorter open reading frame (ORF), corresponding to aa 173–339 (the ORF is identical to AK315956). The short isoform exhibits similar cellular distribution and translocates to ER-PM regions after SOCE activation, similar to the full-length protein (Figure S5A). To elucidate the potential differential roles played by either the luminal or the cytosolic domains of SARAF, we created YFP fusions with either N-terminal (aa 1–191) or C-terminal (aa 196–339) domains and tested their ability to regulate SOCE. We repeated the same experimental paradigm as in Figure 2D and measured SOCE under both store refilling and nonrefilling conditions. Remarkably, truncation of SARAF C-terminal cytosolic domain eliminated SOCE modulation. In contrast, truncation of SARAF luminal N-terminal domain resulted in strong inhibition of SOCE that exhibited little dependence on store refilling (Figure 4A). To further address this issue we measured I_{CRAC} currents in the absence of store refilling in cells expressing C′-SARAF using the same experimental conditions as in Figure 2C. Strikingly, in the absence of store refilling, in cells expressing C′-SARAF isoform currents inactivated to 20.8% ± 2.8% of peak levels,

whereas in control cells the extent of current inactivation was more than 3-fold lower (64.6% ± 5.2%, Figure 4B). Peak current densities were similar in both control-expressing (31 ± 1.4 pA/pF, n = 14) and C′-SARAF- expressing (29 ± 2.3 pA/pF, n = 8) cells, indicating that SOCE inactivation by the C′-SARAF remained dependent on cytosolic Ca^{2+}. To test whether the C′-SARAF interacts directly with STIM1 or Orai1, we performed immuno-pull down analysis by using purified YFP-C′-SARAF (aa 196–339) and extracts from HEK293-T cells coexpressing STIM1 and Orai1-HA. We found that YFP-C′-SARAF mainly precipitated STIM1; traces of Orai1 immunopercipitate were also detected, which may be attributed to its native interaction with STIM1 (Figure 4C). In contrast, similar immuno-pull down analysis using N′-SARAF-YFP were inconclusive and indicated a very weak, if any, interaction with STIM1 (Figure S5F). From the above functional assays, it was expected that C′-SARAF would colocalize at ER-PM junctions upon store depletion in a STIM1-dependnet manner. Indeed, cells expressing both YFP-C′-SARAF and mCherry-Orai1 exhibited dispersed cytosolic staining that did not overlap with that of mCherry-Orai1 (Figure 4D). In contrast, when STIM1 was also coexpressed, YFP-C′-SARAF could be found in reticular structures that moved close to plasma membrane regions upon store depletion to form the classical puncta as described in Figure 3B (see also Figure 4D). The reticular like structures of YFP-C′-SARAF colocalized with STIM1-mCherry, and formation of these structures did not require Orai1 (Figures S5C–S5E). Taken together, the above results suggests that the SARAF C-terminal domain recognizes a domain on STIM1 that enables it to control SOCE activity, whereas the luminal N-terminal domain is responsible for the regulation of SARAF inhibitory activity. To further test this hypothesis, we mutated a conserved glutamate (E148) in the N-terminal region of SARAF and tested its effect on SARAF activity. SARAF(E148A) dominantly inactivated SARAF phenotypic activity both on SOCE and on NFAT translocation (Figures 4E–4G), similar to the phenotype seen after its silencing with siRNA. Moreover, the SARAF(E148A)-YFP mutant exhibited normal translocation into Orai1 puncta at ER-plasma membrane junctions upon store depletion (Figure S5B).

SARAF Associates with STIM1 at Rest

To further test the mode of interaction between SARAF and STIM1, we coexpressed SARAF-GFP and STIM1-mCherry and used a FRET (Förster resonance energy transfer)-based approach to test for intermolecular interactions between the two proteins. Remarkably, resting cells without SOCE stimulation, exhibited a significant FRET signal between SARAF-GFP and STIM1-mCherry. The specificity of this signal was validated in several ways. First, to check for random collisions that may occur between the two constructs, we replaced the donor SARAF-GFP with a cytosolic expressed GFP. Under these conditions, no FRET could be detected between GFP and STIM1-mCherry (Figures 5A and 5B). Next, to test whether true donor and acceptor interactions were responsible for the FRET signal within the oligomer, we coexpressed SARAF-GFP with STIM1-mCherry and added untagged SARAF to compete with SARAF-GFP on STIM1-mCherry binding. Adding untagged SARAF resulted in a decrease in the FRET signal between SARAF-GFP and STIM1-mCherry (Figure 5C). Likewise, the reverse competition with untagged STIM1, underlining the specific interaction between the two molecules. Finally, acceptor photobleaching was used to verify that indeed, destruction of the acceptor dequench donor fluorescence (Figures S6A and S6B) (Riven et al., 2003). Furthermore, independent measurements of FRET were also obtained using the time-domain approach, by measuring fluorescent donor life-time changes, fluorescence lifetime imaging microscopy (FLIM) (Raveh et al., 2010) (Figures S6C–S6F). These measurements verified our initial observation and confirmed that STIM1 and SARAF interact at rest. We then measured FRET changes during SOCE activation after the application of a combination of ATP, Carb, and Tg to cells that express SARAF-GFP and STIM1-mCherry in the presence or absence of Orai1. Remarkably, about a 20% FRET change in the mCherry/GFP ratio was observed only in cells that contained both STIM1 and Orai1 (Figure 5D). The increase in FRET between STIM1 and SARAF after store depletion was reversible when the stores were allowed to refill (Figures S6E and S6F). These results indicate that SARAF and STIM1 associate under resting conditions and that SOCE activation promotes molecular rearrangements between STIM1 and SARAF C termini in an Orai1-dependent manner.

SARAF Inhibits Spontaneous Activation of STIM1

In order to study the functional consequences of STIM1 and SARAF interaction under resting conditions, we silenced endogenous SARAF expression and analyzed STIM1 and Orai1 activity and distribution. In control cells under resting conditions, we observed a reticular staining pattern for YFP-STIM1 that was also evident, in part, near plasma membrane regions with a uniform Orai1-mCherry plasma membrane staining. After ER depletion, this morphology changed into intense colocalized punctate fluorescence signals from both YFP-STIM1 and Orai1-mCherry at plasma membrane regions (Figure 6A). When cells where endogenous SARAF expression was reduced were at rest, YFP-STIM1 fluorescence near the plasma membrane was significantly increased with both STIM1-YFP and Orai1-mCherry forming fluorescent puncta (Figure 6A). After the depletion of Ca^{2+} from the ER by Tg, a smaller additional recruitment of YFP-STIM1 into puncta was apparent but with an overall effect that was similar to control cells under similar conditions. To test the functional consequences of this effect on SOCE, we measured NFAT translocation and $[Ca^{2+}]_{cyto}$ levels under similar conditions. Basal $[Ca^{2+}]_{cyto}$ was significantly elevated in siSARAF-treated cells, a difference that could be reversed by either rescuing SARAF expression by mSARAF or by omitting external Ca^{2+} from the incubation medium (Figure 6C). In agreement with the increased basal SOCE, enhanced nuclear localization of NFAT was also observed in siSARAF-treated cells under either basal conditions or after reversal depletion of the stores (Figure 6D).

SARAF Enhances STIM1 Deoligomerization upon Store Refilling

To gain further insight into the mechanism by which SARAF modulates SOCE, we raised the question whether STIM1-STIM1 oligomeric interactions that underlie SOCE activation

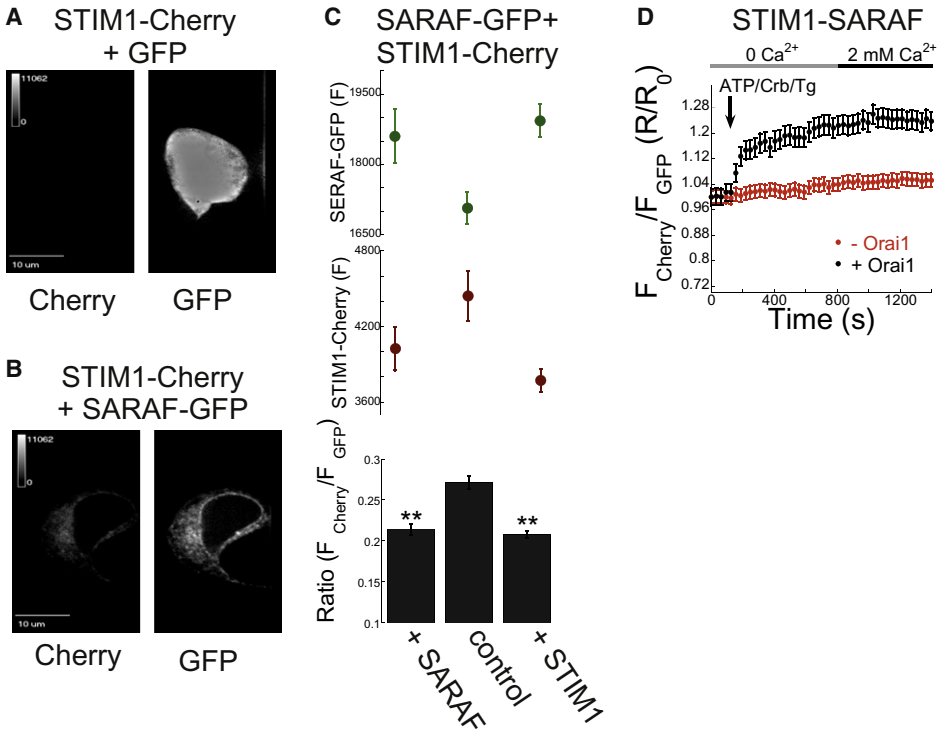

Figure 5. Resting and Dynamic Interaction of SARAF with STIM1

(A and B) Fluorescent images of HEK293-T cells expressing STIM1-mCherry together with GFP (A) or with SARAF-GFP (B). Images are of the same field in both GFP and mCherry channels acquired simultaneously. Fluorescent signals in the mCherry channel result specifically from FRET between SARAF-GFP and STIM1-mCherry (B).

(C) Quantitation of mCherry and GFP fluorescence levels and mCherry/GFP ratios measured from individual cells expressing STIM1-mCherry and SARAF-GFP (n = 232), alone or with untagged STIM1 (n = 120) or SARAF (n = 86).

(D) Time course of mean mCherry/GFP ratios measured from individual cells expressing STIM1-mCherry and SARAF-GFP alone (red, n = 18) or with Orai1 (black, n = 44) after the application of ATP, Carb (100 μM each) and Tg (0.2 μM). p value: ** < 0.01.

and inactivation, are affected by the presence of SARAF. For this purpose, we expressed STIM1-GFP, STIM1-mCherry, and Orai1 with or without SARAF and monitored the dynamics of FRET signals between STIM1-GFP/mCherry during ER Ca^{2+} depletion and refilling. In agreement with previous studies (Liou et al., 2007), we observed an increase in FRET after ER Ca^{2+} depletion and a subsequent decrease after ER Ca^{2+} refilling. In both control and SARAF overexpressing cells, the rate of FRET increase during ER Ca^{2+} depletion and decrease after refilling were similar. With or without SARAF after ER refilling, the time constants of FRET decrease were $11.9*10^{-3} \pm 0.6*10^{-3}$% /s and $12.9*10^{-3} \pm 0.7*10^{-3}$%/s, respectively. In contrast, the extent to which the FRET signal was decreased was different, possibly reflecting a reduced amount of STIM1 oligomers in the presence of SARAF (Figure 7A). Because the extent of ER Ca^{2+} refilling mirrors the oligomeric state of STIM1 (Shen et al., 2011), these results are in apparent contradiction with reduced I_{CRAC} monitored in SARAF-expressing cells. To test this theoretical discrepancy, we determined the levels of ER Ca^{2+} levels under the same experimental conditions as in Figure 7A. Results from this analysis indicated that in agreement with reduced I_{CRAC} and prior to the onset of the STIM1 deoligomerization process, $[Ca^{2+}]_{ER}$ was stabilized at lower levels in cells overexpressing SARAF compared to the levels in control cells (Figure 7B). In conclusion, these results indicate that SARAF reduces active STIM1 oligomers upon Ca^{2+} entry and store refilling even at lower $[Ca^{2+}]_{ER}$ (Figures 7C and 7D).

DISCUSSION

By screening for genes that shape mitochondrial Ca^{2+} levels, we serendipitously identified SARAF as a regulator of store operated calcium influx. Increasing or decreasing SARAF expression levels resulted in opposite effects on global levels of intracellular Ca^{2+} at resting and activated states, indicating an important role for this gene product in the regulation of cellular Ca^{2+} homeostasis. SARAF shares similar topology and overall structure-function relationships with STIM proteins and consists of a single pass ER membrane protein with a cytosolic facing segment responsible for activity, whereas its luminal facing segment engages in regulatory function. Moreover, like STIM1, SARAF also contains a serine-proline rich domain followed by a cluster of basic residues at its C-terminal tail that may aid its interaction with the plasma membrane phospholipids (Huang et al., 2006; Korzeniowski et al., 2009; Park et al., 2009) (Figure 1A). Whether this similarity bears functional significance is currently unclear;

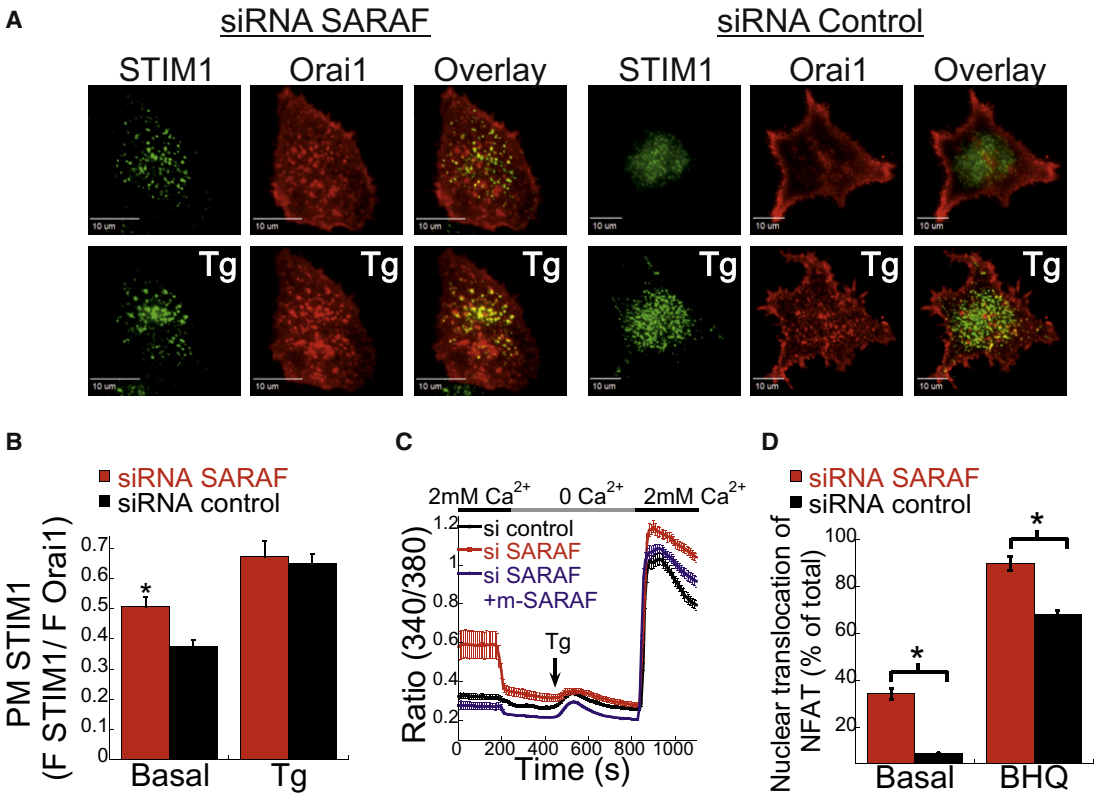

Figure 6. SARAF inhibits basal activation of SOCE

(A) Representative TIRF images of cells treated with siSARAF or siControl, before and after treatment with Tg (bottom).

(B) Quantitation cell surface puncta formed by STIM1-YFP and mCherry-Orai1 in cells treated with siSARAF (n = 24) or with siControl (n = 25), before and after the application of Tg (0.2 μM).

(C) Average of intracellular Ca^{2+} traces of HeLa cells transfected with siSARAF (n = 20), siSARAF+cDNA of mSARAF (n = 38) and siControl (n = 30).

(D) Summary of nuclear localization of GFP-NFAT in siControl or siSARAF-treated cells, before and after BHQ application. Data obtained from three independent experiments, 60–100 cells each. p value: * < 0.05.

however, our results strongly suggest that STIM is the major target for SARAF regulation. This conclusion is supported by several lines of evidence, as both proteins colocalize to the same organelle where they reside within a short distance from each other (5–10 nm) and undergo dynamic physical interaction in response to Ca^{2+} store depletion. The results presented in this work, however, do not rule out additional functional interaction between SARAF and Orai1, and further studies are needed to address this point.

SARAF is expressed in the ER membrane and regulates cellular Ca^{2+} influx mediated by STIM1 activation of Orai1. SARAF regulation over SOCE, however, is largely dependent on Ca^{2+} entry. The robust ability and the nature by which SARAF regulates I_{CRAC} currents is in favor of the idea that SARAF may be part of the molecular entity responsible for one form of slow Ca^{2+}-dependent inactivation process that was previously identified in cultured cells and native tissues (Louzao et al., 1996; Parekh, 1998; Zweifach and Lewis, 1995). Previous studies that analyzed slow Ca^{2+}-dependent inactivation of I_{CRAC} yielded somewhat different findings. In rat basophilic leukemia (RBL) cells inactivation onset depended on cytosolic Ca^{2+}, but no appreciable involvement of store refilling was observed. In Jurkat cells, however, a strong dependence on cytosloic Ca^{2+} for CRAC channel inactivation was also reported, but about 50% of inactivation was traced to the refilling of stores. Similar to the findings in both studies mentioned above, we find that the onset of CRAC channel inactivation mediated by SARAF critically depends on cytosolic Ca^{2+}. Involvement of store refilling, however, is only apparent with the full-length SARAF but not with its short splice isoform. Moreover, we find that the depletion of SARAF expression in Jurkat T cells also diminishes I_{CRAC} inactivation (Figure 2H). It is therefore conceivable that differential cell-specific alternative splicing of SARAF may explain some of the discrepancies observed in previous studies and thus may also underlie a mechanism for regulating cell Ca^{2+} homeostasis at the posttranscriptional level.

The precise molecular mechanism that underlies the ability of SARAF to sense cytosolic Ca^{2+} elevations and induce I_{CRAC} inactivation is unclear at this stage. Recently, via a proteomics approach, a modulator for SOCE activity, an EF-hand containing a cytosolic protein termed CRACR2A, was identified (Srikanth et al., 2010). CRACR2A binds both Orai1 and STIM1 to aid the stabilization of the active CRAC complexes, mainly under conditions of low abundance of STIM1 and Orai1. Upon the elevation of cytosolic Ca^{2+}, CRACR2A is believed to dissociate from the

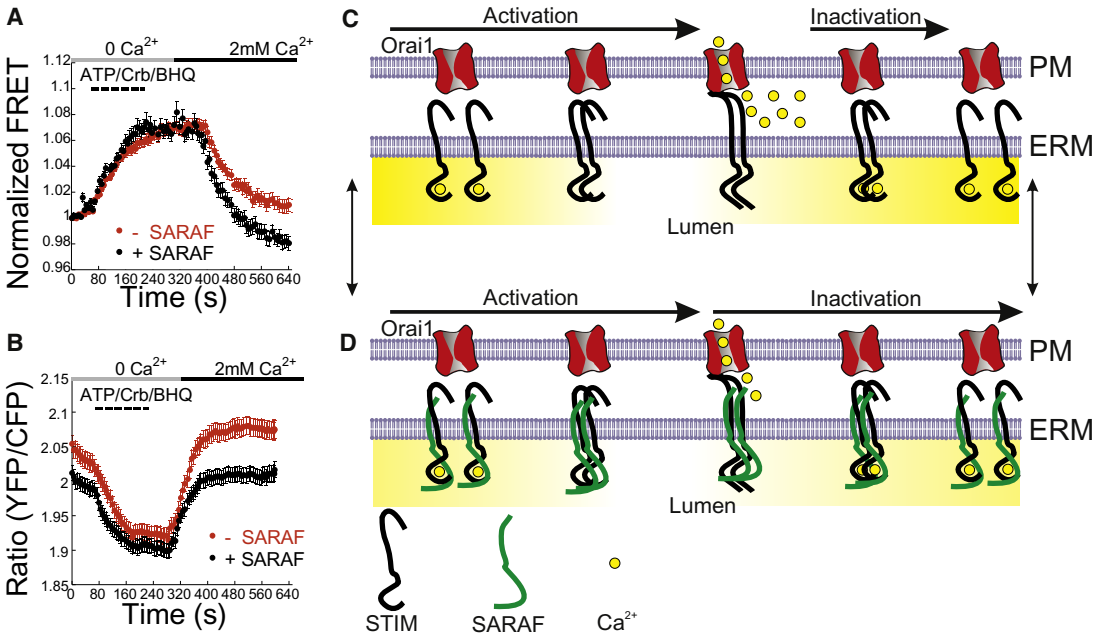

Figure 7. SARAF Enhances STIM1 Disaggregation after Store Refilling

(A) Time course of mean GFP/mCherry FRET signal measured from individual cells expressing Orai1, STIM1-mCherry and STIM1-GFP alone (n = 41) or with SARAF (n = 21). SOCE was induced by ATP, Carb (100 μM each) and BHQ (2 μM).

(B) Dynamics of ER Ca^{2+} levels measured using D1ER fluorescence ratio of individual cells expressing Orai1, STIM1, D1ER alone (n = 211), or with SARAF (n = 189), SOCE induction like in (A) and store refilling by the application of 2 mM Ca^{2+}.

(C and D) Cartoons depicting the action of SARAF on SOCE activity. (C) Upon Ca^{2+} depletion from the ER (depicted as a yellow gradient in the ER lumen), the EF hand of STIM molecules (residing in the ER membrane, ERM) lose their Ca^{2+} bound ions (yellow balls). The dissociation of Ca^{2+} ions promotes the dimerization/aggregation of STIM molecules and to induce a conformational rearrangement of the C terminal of STIM enabling their interaction with Orai channels at the plasma membrane (PM). STIM-Orai interaction promotes channel activation and entry of Ca^{2+} ions into the cell. After refilling of the ER with the entering Ca^{2+} ions by SERCA (not shown), Ca^{2+} levels in the ER lumen rise to reverse the above process. In the absence of SARAF (green) the reverse process is less efficient to cause elevation in intracellular Ca^{2+} concentration above normal levels. (D), SARAF association with STIM proteins affect the above process by facilitating the disaggregation of STIM molecules to efficiently turn off Orai when the ER lumen is filled with the appropriate Ca^{2+} levels, and thus preventing the overload of the cell with excessive Ca^{2+} ions. Events read left to right.

complex to promote the destabilization of the SOCE complex. Like SARAF it also responds to local elevation of Ca^{2+} near the plasma membrane. It remains to be seen if CRACR2A has a corresponding effect on I_{CRAC}. Whether the two proteins are part of the same protein complex that regulates CRAC channels is an appealing possibility that awaits future studies.

The ER luminal facing segment of SARAF regulates the inhibitory action mediated by the cytosolic facing segment, which has the capability to interact with the C-terminal cytosolic domain of STIM1. The apparent action of SARAF in facilitating ER Ca^{2+} refilling-dependent inactivation is, however, likely a consequence of its ability to indirectly respond to changes in $[Ca^{2+}]_{ER}$ and promote an efficient disaggregation of STIM molecules (Figure 7). The regulatory role of the SARAF ER luminal facing domain is underlined by the enhanced ability of the short isoform of SARAF to inhibit I_{CRAC} independently of store refilling. The fact that a mutation in this region has a dominant negative effect on SOCE activity also suggests that SARAF may be functional as a dimer or in a higher-order complex. The ER luminal facing segment of SARAF, however, does not show clear similarity with any known Ca^{2+} binding motifs. In addition, I_{CRAC} measurements in the absence or presence of store refilling yield similar ~2-fold differences in both control and SARAF-expressing cells (Figures 2A and S2C), and translocation of SARAF to ER-PM regions depends on that of STIM1 but not on store depletion per se (Figure 3). It is therefore less likely that SARAF directly binds Ca^{2+} ions and thus raises the possibility that SARAF may respond to changes in $[Ca^{2+}]_{ER}$ indirectly through interaction with STIM or other ER Ca^{2+}-sensitive proteins or is regulated by other physiological mechanisms (Enyedi et al., 2010; Hawkins et al., 2010). The functional interaction of SARAF with STIM1 may point toward the former possibility, were coupling between STIM1 Ca^{2+} occupancy and the SARAF inhibitory mode, found to occur. Such a scenario is in agreement with spontaneous activation of STIM1 proteins without ER Ca^{2+} depletion, observed after knockdown of SARAF expression or with a more efficient disaggregation and stabilization of inactive STIM1 proteins at lower ER Ca^{2+} levels, after an increase in SARAF expression. The direct mode by which SARAF affects SOCE inactivation after ER Ca^{2+} refilling is currently unresolved and awaits future studies.

Although no direct evidence provided to date shows that mutations in SARAF are linked to any disease state in humans, studies employing various differential expression or transcriptome-profiling strategies have recently identified SARAF as a

biomarker linked to prostate cancer (Romanuik et al., 2009a), Alzheimer's disease (Twine et al., 2011), and dilated cardiomyopathy (DCM) (Camargo and Azuaje, 2008). Notably, most of these disease states are accompanied by abnormal intracellular Ca^{2+} handling. It is also interesting to note that both STIM1 and SARAF transcripts have been shown to be positively modulated by androgens, implying common regulatory mechanisms of these genes expression levels (Berry et al., 2011; Romanuik et al., 2009b).

In summary we have identified the gene product of *TMEM66*, SARAF, as a regulator of store operated calcium entry. SARAF promotes slow I_{CRAC} inactivation after Ca^{2+} entry and refilling of the endoplasmic reticulum. This physiological role places SARAF as a dominant player in a protective mechanism designed to prevent rapid overfilling of cells with Ca^{2+} ions.

EXPERIMENTAL PROCEDURES

Fluorescent Measurements of Intracellular Ions

Typically, 6–8 hr after plasmid transfection and 17–24 hr before starting the experiments, cells were plated onto 24 mm cover glass coated with L-polylysine. On the day of the experiments, the cover glass was mounted on an imaging chamber and washed with Ringer solution. Fura-2 loading of cells was performed as previously described (Palty et al., 2010). Cytosolic Ca^{2+} levels were recorded from fura-2 loaded cells, excited at wavelengths of 340/20 and 380/20 nm and imaged with 510/80 nm filters.

Mitochondrial Ca^{2+} levels were monitored in cells expressing the mitochondrial-targeted ratiometric-pericam (RP-mt) protein via excitation wavelengths of 436/20 nm and 480/20 nm and emission collected with a 540/80 nm filter. Endoplasmic reticulum Ca^{2+} levels were recorded in cells expressing D1ER via a dual view device with a CFP/YFP filter set.

All experiments were conducted with Ringer's solutions containing 130 mM NaCl, 20 mM HEPES,15 mM Glucose, 5 mM KCl, and 0.8 mM $MgCl_2$ with the pH adjusted to 7.4. Ringer's solution was supplemented with 2 mM $CaCl_2$ or 1 mM EGTA (Ca^{2+} free) as indicated. For all single cell imaging experiments, traces of averaged responses, recorded from 10 to 50 cells in each experiment, were plotted with KaleidaGraph. All experiments were repeated 2 to 8 times. Statistical significance was determined with t test analysis; $p < 0.05$ was considered significant. All data are shown as average ± SEM.

NFAT Translocation Assay

Monitoring of nuclear translocation of NFAT-GFP was performed 30–48 hr posttransfection in HEK293-T or HeLa cells. At the start of each experiment, cells were washed twice with Ca^{2+}-free Ringer's solution, and 2 μM BHQ or 0.2 μM Tg were added for 5 min. Cells were then washed with Ca^{2+}-free Ringer's solution for additional 5 min and incubated for 30 min in a 2 mM Ca^{2+}-containing Ringer's solution. Localization of NFAT-GFP in cells was examined by fluorescent microscopy before and after SOCE induction.

Electrophysiological Recordings

Recorded HEK293-T or HEK293 cells were transfected 24–36 hr prior to electrophysiology experiments. Each transfection contained STIM1 and Orai1 with or without SARAF (1 μg each). Cells were transferred to the measurement chamber more than 6 hr before measurements for HEK293 cells and 10–20 min for Jurkat cells. Membrane currents were recorded under voltage-clamp conditions with whole-cell variation of the patch-clamp configuration by using Axopatch 200B (Axon Instruments). Patch pipettes were fabricated from borosilicate glass capillaries (2–5 MΩ). Signals were analog filtered with a 1 kHz low-pass Bessel filter. Data acquisition and analysis were done with pCLAMP 9 software (Axon Instruments). All data were leak-corrected with the current elicited in Ca^{2+}-free Ringer's solution at the beginning of each experiment. More detailed information and solutions used are in Extended Experimental Procedures.

ACCESSION NUMBERS

The GeneBank accession number for SARAF is JQ348891, and for SARAF short isoform it is JQ348892.

SUPPLEMENTAL INFORMATION

Supplemental Information includes Extended Experimental Procedures, six figures, and one movie and can be found with this article online at doi:10.1016/j.cell.2012.01.055.

ACKNOWLEDGMENTS

The authors would like to thank Elisha Shalgi for technical help and Dr. Dan Minor for his helpful comments and critical reading of the manuscript. The work was supported in part by the Clore postdoctoral fellowship (RP), the Josef Cohn Center for Biomembrane Research, The Israeli Science Foundation (ISF grant 207/09) and the Minerva Foundation (Munich) all to ER.

Received: July 15, 2011
Revised: November 24, 2011
Accepted: January 26, 2012
Published online: March 29, 2012

REFERENCES

Baba, Y., Hayashi, K., Fujii, Y., Mizushima, A., Watarai, H., Wakamori, M., Numaga, T., Mori, Y., Iino, M., Hikida, M., and Kurosaki, T. (2006). Coupling of STIM1 to store-operated Ca2+ entry through its constitutive and inducible movement in the endoplasmic reticulum. Proc. Natl. Acad. Sci. USA *103*, 16704–16709.

Barr, V.A., Bernot, K.M., Srikanth, S., Gwack, Y., Balagopalan, L., Regan, C.K., Helman, D.J., Sommers, C.L., Oh-Hora, M., Rao, A., and Samelson, L.E. (2008). Dynamic movement of the calcium sensor STIM1 and the calcium channel Orai1 in activated T-cells: puncta and distal caps. Mol. Biol. Cell *19*, 2802–2817.

Berry, P.A., Birnie, R., Droop, A.P., Maitland, N.J., and Collins, A.T. (2011). The calcium sensor STIM1 is regulated by androgens in prostate stromal cells. Prostate *71*, 1646–1655.

Bird, G.S., Hwang, S.Y., Smyth, J.T., Fukushima, M., Boyles, R.R., and Putney, J.W., Jr. (2009). STIM1 is a calcium sensor specialized for digital signaling. Curr. Biol. *19*, 1724–1729.

Brandman, O., Liou, J., Park, W.S., and Meyer, T. (2007). STIM2 is a feedback regulator that stabilizes basal cytosolic and endoplasmic reticulum Ca2+ levels. Cell *131*, 1327–1339.

Cahalan, M.D. (2009). STIMulating store-operated Ca(2+) entry. Nat. Cell Biol. *11*, 669–677.

Camargo, A., and Azuaje, F. (2008). Identification of dilated cardiomyopathy signature genes through gene expression and network data integration. Genomics *92*, 404–413.

Derler, I., Fahrner, M., Muik, M., Lackner, B., Schindl, R., Groschner, K., and Romanin, C. (2009). A Ca2(+)release-activated Ca2(+) (CRAC) modulatory domain (CMD) within STIM1 mediates fast Ca2(+)-dependent inactivation of ORAI1 channels. J. Biol. Chem. *284*, 24933–24938.

Enyedi, B., Várnai, P., and Geiszt, M. (2010). Redox state of the endoplasmic reticulum is controlled by Ero1L-alpha and intraluminal calcium. Antioxid. Redox Signal. *13*, 721–729.

Feske, S., Gwack, Y., Prakriya, M., Srikanth, S., Puppel, S.H., Tanasa, B., Hogan, P.G., Lewis, R.S., Daly, M., and Rao, A. (2006). A mutation in Orai1 causes immune deficiency by abrogating CRAC channel function. Nature *441*, 179–185.

Frischauf, I., Muik, M., Derler, I., Bergsmann, J., Fahrner, M., Schindl, R., Groschner, K., and Romanin, C. (2009). Molecular determinants of the

coupling between STIM1 and Orai channels: differential activation of Orai1-3 channels by a STIM1 coiled-coil mutant. J. Biol. Chem. *284*, 21696–21706.

Hardie, R.C., and Minke, B. (1993). Novel Ca2+ channels underlying transduction in Drosophila photoreceptors: implications for phosphoinositide-mediated Ca2+ mobilization. Trends Neurosci. *16*, 371–376.

Hawkins, B.J., Irrinki, K.M., Mallilankaraman, K., Lien, Y.C., Wang, Y., Bhanumathy, C.D., Subbiah, R., Ritchie, M.F., Soboloff, J., Baba, Y., et al. (2010). S-glutathionylation activates STIM1 and alters mitochondrial homeostasis. J. Cell Biol. *190*, 391–405.

Hogan, P.G., Lewis, R.S., and Rao, A. (2010). Molecular basis of calcium signaling in lymphocytes: STIM and ORAI. Annu. Rev. Immunol. *28*, 491–533.

Hoth, M., and Penner, R. (1993). Calcium release-activated calcium current in rat mast cells. J. Physiol. *465*, 359–386.

Huang, G.N., Zeng, W., Kim, J.Y., Yuan, J.P., Han, L., Muallem, S., and Worley, P.F. (2006). STIM1 carboxyl-terminus activates native SOC, I(crac) and TRPC1 channels. Nat. Cell Biol. *8*, 1003–1010.

Kawasaki, T., Lange, I., and Feske, S. (2009). A minimal regulatory domain in the C terminus of STIM1 binds to and activates ORAI1 CRAC channels. Biochem. Biophys. Res. Commun. *385*, 49–54.

Kiselyov, K., Xu, X., Mozhayeva, G., Kuo, T., Pessah, I., Mignery, G., Zhu, X., Birnbaumer, L., and Muallem, S. (1998). Functional interaction between InsP3 receptors and store-operated Htrp3 channels. Nature *396*, 478–482.

Korzeniowski, M.K., Popovic, M.A., Szentpetery, Z., Varnai, P., Stojilkovic, S.S., and Balla, T. (2009). Dependence of STIM1/Orai1-mediated calcium entry on plasma membrane phosphoinositides. J. Biol. Chem. *284*, 21027–21035.

Lee, K.P., Yuan, J.P., Zeng, W., So, I., Worley, P.F., and Muallem, S. (2009). Molecular determinants of fast Ca2+-dependent inactivation and gating of the Orai channels. Proc. Natl. Acad. Sci. USA *106*, 14687–14692.

Lewis, R.S. (2007). The molecular choreography of a store-operated calcium channel. Nature *446*, 284–287.

Liou, J., Kim, M.L., Heo, W.D., Jones, J.T., Myers, J.W., Ferrell, J.E., Jr., and Meyer, T. (2005). STIM is a Ca2+ sensor essential for Ca2+-store-depletion-triggered Ca2+ influx. Curr. Biol. *15*, 1235–1241.

Liou, J., Fivaz, M., Inoue, T., and Meyer, T. (2007). Live-cell imaging reveals sequential oligomerization and local plasma membrane targeting of stromal interaction molecule 1 after Ca2+ store depletion. Proc. Natl. Acad. Sci. USA *104*, 9301–9306.

Litjens, T., Harland, M.L., Roberts, M.L., Barritt, G.J., and Rychkov, G.Y. (2004). Fast Ca(2+)-dependent inactivation of the store-operated Ca2+ current (ISOC) in liver cells: a role for calmodulin. J. Physiol. *558*, 85–97.

Liu, X., Cheng, K.T., Bandyopadhyay, B.C., Pani, B., Dietrich, A., Paria, B.C., Swaim, W.D., Beech, D., Yildrim, E., Singh, B.B., et al. (2007). Attenuation of store-operated Ca2+ current impairs salivary gland fluid secretion in TRPC1(-/-) mice. Proc. Natl. Acad. Sci. USA *104*, 17542–17547.

Louzao, M.C., Ribeiro, C.M., Bird, G.S., and Putney, J.W., Jr. (1996). Cell type-specific modes of feedback regulation of capacitative calcium entry. J. Biol. Chem. *271*, 14807–14813.

Muik, M., Frischauf, I., Derler, I., Fahrner, M., Bergsmann, J., Eder, P., Schindl, R., Hesch, C., Polzinger, B., Fritsch, R., et al. (2008). Dynamic coupling of the putative coiled-coil domain of ORAI1 with STIM1 mediates ORAI1 channel activation. J. Biol. Chem. *283*, 8014–8022.

Mullins, F.M., Park, C.Y., Dolmetsch, R.E., and Lewis, R.S. (2009). STIM1 and calmodulin interact with Orai1 to induce Ca2+-dependent inactivation of CRAC channels. Proc. Natl. Acad. Sci. USA *106*, 15495–15500.

Navarro-Borelly, L., Somasundaram, A., Yamashita, M., Ren, D., Miller, R.J., and Prakriya, M. (2008). STIM1-Orai1 interactions and Orai1 conformational changes revealed by live-cell FRET microscopy. J. Physiol. *586*, 5383–5401.

Palmer, A.E., Jin, C., Reed, J.C., and Tsien, R.Y. (2004). Bcl-2-mediated alterations in endoplasmic reticulum Ca2+ analyzed with an improved genetically encoded fluorescent sensor. Proc. Natl. Acad. Sci. USA *101*, 17404–17409.

Palty, R., Silverman, W.F., Hershfinkel, M., Caporale, T., Sensi, S.L., Parnis, J., Nolte, C., Fishman, D., Shoshan-Barmatz, V., Herrmann, S., et al. (2010). NCLX is an essential component of mitochondrial Na+/Ca2+ exchange. Proc. Natl. Acad. Sci. USA *107*, 436–441.

Pani, B., Ong, H.L., Brazer, S.C., Liu, X., Rauser, K., Singh, B.B., and Ambudkar, I.S. (2009). Activation of TRPC1 by STIM1 in ER-PM microdomains involves release of the channel from its scaffold caveolin-1. Proc. Natl. Acad. Sci. USA *106*, 20087–20092.

Parekh, A.B. (1998). Slow feedback inhibition of calcium release-activated calcium current by calcium entry. J. Biol. Chem. *273*, 14925–14932.

Parekh, A.B., and Putney, J.W., Jr. (2005). Store-operated calcium channels. Physiol. Rev. *85*, 757–810.

Park, C.Y., Hoover, P.J., Mullins, F.M., Bachhawat, P., Covington, E.D., Raunser, S., Walz, T., Garcia, K.C., Dolmetsch, R.E., and Lewis, R.S. (2009). STIM1 clusters and activates CRAC channels via direct binding of a cytosolic domain to Orai1. Cell *136*, 876–890.

Peinelt, C., Vig, M., Koomoa, D.L., Beck, A., Nadler, M.J., Koblan-Huberson, M., Lis, A., Fleig, A., Penner, R., and Kinet, J.P. (2006). Amplification of CRAC current by STIM1 and CRACM1 (Orai1). Nat. Cell Biol. *8*, 771–773.

Prakriya, M., Feske, S., Gwack, Y., Srikanth, S., Rao, A., and Hogan, P.G. (2006). Orai1 is an essential pore subunit of the CRAC channel. Nature *443*, 230–233.

Putney, J.W., Jr. (1986). A model for receptor-regulated calcium entry. Cell Calcium *7*, 1–12.

Raveh, A., Cooper, A., Guy-David, L., and Reuveny, E. (2010). Nonenzymatic rapid control of GIRK channel function by a G protein-coupled receptor kinase. Cell *143*, 750–760.

Ríos, E. (2010). The cell boundary theorem: a simple law of the control of cytosolic calcium concentration. J. Physiol. Sci. *60*, 81–84.

Riven, I., Kalmanzon, E., Segev, L., and Reuveny, E. (2003). Conformational rearrangements associated with the gating of the G protein-coupled potassium channel revealed by FRET microscopy. Neuron *38*, 225–235.

Romanuik, T.L., Ueda, T., Le, N., Haile, S., Yong, T.M., Thomson, T., Vessella, R.L., and Sadar, M.D. (2009a). Novel biomarkers for prostate cancer including noncoding transcripts. Am. J. Pathol. *175*, 2264–2276.

Romanuik, T.L., Wang, G., Holt, R.A., Jones, S.J., Marra, M.A., and Sadar, M.D. (2009b). Identification of novel androgen-responsive genes by sequencing of LongSAGE libraries. BMC Genomics *10*, 476.

Roos, J., DiGregorio, P.J., Yeromin, A.V., Ohlsen, K., Lioudyno, M., Zhang, S., Safrina, O., Kozak, J.A., Wagner, S.L., Cahalan, M.D., et al. (2005). STIM1, an essential and conserved component of store-operated Ca2+ channel function. J. Cell Biol. *169*, 435–445.

Shen, W.W., Frieden, M., and Demaurex, N. (2011). Local cytosolic Ca2+ elevations are required for stromal interaction molecule 1 (STIM1) de-oligomerization and termination of store-operated Ca2+ entry. J. Biol. Chem. *286*, 36448–36459.

Soboloff, J., Spassova, M.A., Tang, X.D., Hewavitharana, T., Xu, W., and Gill, D.L. (2006). Orai1 and STIM reconstitute store-operated calcium channel function. J. Biol. Chem. *281*, 20661–20665.

Srikanth, S., Jung, H.J., Kim, K.D., Souda, P., Whitelegge, J., and Gwack, Y. (2010). A novel EF-hand protein, CRACR2A, is a cytosolic Ca2+ sensor that stabilizes CRAC channels in T cells. Nat. Cell Biol. *12*, 436–446.

Stathopulos, P.B., Zheng, L., Li, G.Y., Plevin, M.J., and Ikura, M. (2008). Structural and mechanistic insights into STIM1-mediated initiation of store-operated calcium entry. Cell *135*, 110–122.

Stathopulos, P.B., Zheng, L., and Ikura, M. (2009). Stromal interaction molecule (STIM) 1 and STIM2 calcium sensing regions exhibit distinct unfolding and oligomerization kinetics. J. Biol. Chem. *284*, 728–732.

Su, A.I., Wiltshire, T., Batalov, S., Lapp, H., Ching, K.A., Block, D., Zhang, J., Soden, R., Hayakawa, M., Kreiman, G., et al. (2004). A gene atlas of the mouse and human protein-encoding transcriptomes. Proc. Natl. Acad. Sci. USA *101*, 6062–6067.

Tomida, T., Hirose, K., Takizawa, A., Shibasaki, F., and Iino, M. (2003). NFAT functions as a working memory of Ca2+ signals in decoding Ca2+ oscillation. EMBO J. *22*, 3825–3832.

Twine, N.A., Janitz, K., Wilkins, M.R., and Janitz, M. (2011). Whole transcriptome sequencing reveals gene expression and splicing differences in brain regions affected by Alzheimer's disease. PLoS ONE *6*, e16266.

Vig, M., Peinelt, C., Beck, A., Koomoa, D.L., Rabah, D., Koblan-Huberson, M., Kraft, S., Turner, H., Fleig, A., Penner, R., and Kinet, J.P. (2006). CRACM1 is a plasma membrane protein essential for store-operated Ca2+ entry. Science *312*, 1220–1223.

Wu, M.M., Buchanan, J., Luik, R.M., and Lewis, R.S. (2006). Ca2+ store depletion causes STIM1 to accumulate in ER regions closely associated with the plasma membrane. J. Cell Biol. *174*, 803–813.

Yeromin, A.V., Zhang, S.L., Jiang, W., Yu, Y., Safrina, O., and Cahalan, M.D. (2006). Molecular identification of the CRAC channel by altered ion selectivity in a mutant of Orai. Nature *443*, 226–229.

Yuan, J.P., Zeng, W., Dorwart, M.R., Choi, Y.J., Worley, P.F., and Muallem, S. (2009). SOAR and the polybasic STIM1 domains gate and regulate Orai channels. Nat. Cell Biol. *11*, 337–343.

Zhang, Z., and Henzel, W.J. (2004). Signal peptide prediction based on analysis of experimentally verified cleavage sites. Protein Sci. *13*, 2819–2824.

Zhang, S.L., Yu, Y., Roos, J., Kozak, J.A., Deerinck, T.J., Ellisman, M.H., Stauderman, K.A., and Cahalan, M.D. (2005). STIM1 is a Ca2+ sensor that activates CRAC channels and migrates from the Ca2+ store to the plasma membrane. Nature *437*, 902–905.

Zhang, S.L., Yeromin, A.V., Zhang, X.H., Yu, Y., Safrina, O., Penna, A., Roos, J., Stauderman, K.A., and Cahalan, M.D. (2006). Genome-wide RNAi screen of Ca(2+) influx identifies genes that regulate Ca(2+) release-activated Ca(2+) channel activity. Proc. Natl. Acad. Sci. USA *103*, 9357–9362.

Zhou, Y., Meraner, P., Kwon, H.T., Machnes, D., Oh-hora, M., Zimmer, J., Huang, Y., Stura, A., Rao, A., and Hogan, P.G. (2010). STIM1 gates the store-operated calcium channel ORAI1 in vitro. Nat. Struct. Mol. Biol. *17*, 112–116.

Zweifach, A., and Lewis, R.S. (1995). Slow calcium-dependent inactivation of depletion-activated calcium current. Store-dependent and -independent mechanisms. J. Biol. Chem. *270*, 14445–14451.